ENHANCEMENT OF HEAT TRANSFER BY THERMOCAPILLARY CONVECTION AROUND BUBBLES — A NUMERICAL STUDY

J. Straub, J. Betz, and R. Marek
Lehrstuhl A für Thermodynamik, Technical University of Munich, Munich, Germany

For a gas bubble floating in a liquid-filled rectangular enclosure, the effect of thermocapillary convection on fluid flow and heat transfer is studied in a cross section with a two-dimensional model. A transient finite difference scheme is applied for the numerical calculations. For a fluid with Pr = 1.93, the overall heat transfer in the liquid is presented for selected configurations in terms of the dimensionless numbers Nu and Ma. Contrary to the common view that an enclosed gas volume would reduce the heat transfer due to its insulating behavior, the energy transport is rather augmented by the thermocapillary convection acting on the free surface. For higher Marangoni numbers, oscillatory flow behavior occurs.

When a free surface is subjected to a temperature gradient, a flow termed Marangoni [1], surface tension driven or thermocapillary convection is induced. Before the first microgravity experiments had been performed, thermocapillary convection was not given much attention, as it was regarded to be negligible in comparison with buoyancy convection. Recently, considerable interest has been shown in thermocapillary flow, especially in materials processing [2–4]. Experiments of subcooled boiling under microgravity conditions [5] clearly demonstrated that Marangoni convection can fully replace the buoyancy-dominated heat transfer mechanisms of Earth's gravity. As space experiments are generally expensive, numerical simulations can help cut costs and facilitate the realization of new experiments.

In some technical systems, it is highly desirable that convection substantially contribute to both heat and mass transfer, while in others, such as building materials, air insulation is used to reduce heat losses. In particular, Marangoni convection can affect floating bubbles or droplets in a liquid exposed to a temperature gradient. Young et al. [6] investigated the motion of bubbles by adjusting a vertical temperature gradient in a fluid in such a way that the buoyancy

Received 6 February 1992; accepted 11 June 1993.

This paper is an excerpt from the diploma thesis of the second author. The first and third authors are supported by the DFG (Deutsche Forschungsgemeinschaft) through grant Str 117/29-1, which is gratefully acknowledged.

Address correspondence to J. Straub, Lehrstuhl A für Thermodynamik, Technical University of Munich, Arcisstraße 21, W-8000 Munich 2, Germany.

Numerical Heat Transfer, Part A, 25:501–518, 1994

1040–7782/94 $10.00 + .00

NOMENCLATURE

a	pressure coefficient	γ	constant
b	mass source	Δt	time step
B	width of the cavity	ΔT	temperature difference in the box ($= T_t - T_b$)
c_p	isobaric specific heat capacity	η	dynamic viscosity
$d\sigma/dT$	temperature coefficient of surface tension	λ	thermal conductivity
Fo	Fourier number ($= \alpha t/L^2$)	μ	universal exponent
g	gravitational acceleration (in y direction)	ν	kinematic viscosity
h, H	height of the cavity	ϱ	density of the liquid
L	characteristic length ($L = H$ for cases M, M − B, M + B; $L = h$ for cases M_b and M_t)	σ	surface tension
		τ	shear stress
		ω_p, ω_v	relaxation factors
Ma	Marangoni number for the box [$= -(d\sigma/dT)(L\,\Delta T/\alpha\eta)$]	**Subscripts**	
Nu	local Nusselt number [$= L[T(y + \Delta y) - T(y)]/(\Delta T\,\Delta y)$]	b	bottom wall
		c	critical
p	pressure	cold	cold wall
Pr	Prandtl number ($= \nu/\alpha = \eta c_p/\lambda$)	g	gas
R	cylinder radius	hot	hot wall
Ra	Rayleigh number for the box ($= g\beta_\varrho\,\Delta T L^3/\nu\alpha$)	l	liquid
		M	Marangoni
Re	Reynolds number for the box ($= w_{max}\varrho L/\eta$)	max	maximum
		nb	neighboring points
S	security factor	osc	oscillation
t	time	P	central point of a control volume
T	temperature	r	radial
u	x velocity	t	top wall
u_t	radial velocity on the cylinder surface	0	reference value for fluid properties [$T_0 = \frac{1}{2}(T_h + T_c)$]
u_φ	azimuthal velocity on the cylinder surface	φ	azimuthal
v	y velocity	**Superscript**	
w_{max}	maximum velocity (for evaluation of the Reynolds number) ($= \max[\|u\| + \|v\|]$)	′	corrective term
		*	estimated term or value for the old time level
α	thermal diffusivity	**	corrected term
β_ϱ	thermal expansion coefficient		

of the bubble was compensated by the Marangoni force. However, the heat transfer was not considered. At first sight, one would expect a gas bubble floating in a liquid to significantly reduce the heat transfer due to its insulating behavior. Taking thermocapillary flow into consideration, the question arises, can heat transfer through a liquid be augmented by inserting a gas bubble?

The aim of our study is to evaluate the heat transfer by thermocapillary convection around a gas bubble, frozen at a definite location in a rectangular enclosure with a vertical temperature gradient. Variable gravity conditions make it possible to study the interaction of buoyancy and surface tension driven convection. Numerical simulations of Marek and Straub [7] revealed that, even under Earth's gravity conditions, Marangoni flow cannot be overcome by natural convec-

tion in certain configurations. Depending on the boundary conditions, thermocapillary flow can either augment or counteract natural convection. Contrary to former assumptions, Marangoni flow is, in general, not negligible.

PHYSICAL MODEL

As a first approximation of the problem of thermocapillary flow in a cross section around an enclosed gas bubble in a liquid with adjacent temperature gradient, the configuration of a rectangular container with an enclosed cylinder of infinite length (Figure 1) is studied. This truncation to two dimensions yields an enormous gain in computing time and memory, while estimations of the enhancement of heat transfer by thermocapillary convection can be transferred to the three-dimensional geometry with bubble.

Furthermore, as the cylinder is assumed to be horizontally centered in the two-dimensional (2D) box and the boundary conditions are symmetrical to the y axis, heat transfer and fluid flow are only computed in the right half of the 2D box (Figure 1).

At a real gas-liquid interface, thermocapillary convection expands both into the gas and into the liquid phase. Due to the relatively small values for the transport properties η and λ and the small density ϱ of the gas, heat transfer and fluid flow are neglected inside the cylinder and are only considered in the liquid as an interaction of Marangoni and natural convection.

CONSERVATION LAWS

The system of an enclosed gas cylinder in a rectangular cavity filled with liquid is governed by the conservation laws for mass, momentum, and energy. Using the Boussinesq approximation [8] for the properties of the surrounding liquid, the following coupled conservation laws apply [9]:

Mass

$$\frac{1}{\varrho_0}\frac{\partial \varrho}{\partial t} + \frac{\partial u}{\partial x} + \frac{\partial v}{\partial y} = 0 \tag{1}$$

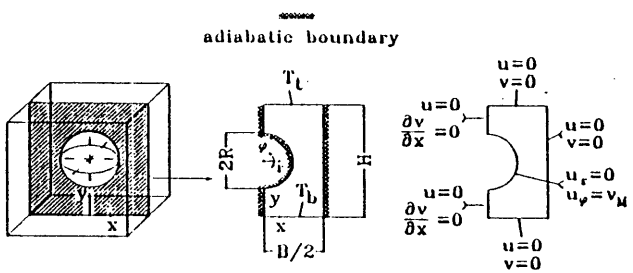

Figure 1. Computational domain in the three-dimensional heat transfer problem with boundary conditions.

Energy

$$\frac{\partial T}{\partial t} + u\frac{\partial T}{\partial x} + v\frac{\partial T}{\partial y} = \alpha_0\left(\frac{\partial^2 T}{\partial x^2} + \frac{\partial^2 T}{\partial y^2}\right) \tag{2}$$

x momentum

$$\frac{\partial u}{\partial t} + u\frac{\partial u}{\partial x} + v\frac{\partial u}{\partial y} = -\frac{1}{\varrho_0}\frac{\partial p}{\partial x} + \nu_0\left(\frac{\partial^2 u}{\partial x^2} + \frac{\partial^2 u}{\partial y^2}\right) \tag{3}$$

y momentum

$$\frac{\partial v}{\partial t} + u\frac{\partial v}{\partial x} + v\frac{\partial v}{\partial y} = -\frac{\varrho(T)}{\varrho_0}g - \frac{1}{\varrho_0}\frac{\partial p}{\partial y} + \nu_0\left(\frac{\partial^2 v}{\partial x^2} + \frac{\partial^2 v}{\partial y^2}\right) \tag{4}$$

INITIAL AND BOUNDARY CONDITIONS

For $t = 0$ the liquid around the gas cylinder is assumed to be at rest:

$$u(x, y, t = 0) = 0 \wedge v(x, y, t = 0) = 0 \tag{5}$$

and a temperature field is chosen constant in the x direction with a constant gradient in the y direction, Eq. (6), as in the case of steady state heat conduction without a gas cylinder.

$$T(x, y, t = 0) = T_b + (T_t - T_b)\frac{y}{L} \tag{6}$$

The governing boundary conditions for the 2D cylinder in the container model of Figure 1 are the thermal and the hydrodynamic boundary conditions.

Thermal Boundary Conditions

As the thermal conductivity of air is small in comparison with that of the surrounding liquid, the surface of the cylinder is assumed to be adiabatic. Moreover, heat transfer by radiation is neglected, since the maximum temperature differences of 3.4 K in the system are small; heat is only transported by conduction and convection in the liquid. The bottom and top walls of the enclosure are kept at constant but different temperatures, while the side walls are assumed to be perfectly insulated:

$$T(y = 0) = T_b \wedge T(y = H) = T_t \wedge \frac{\partial T}{\partial x} = 0\Big|_{r = 0,\, x = B/2} \wedge \frac{\partial T}{\partial r} = 0\Big|_{r = R} \tag{7}$$

Hydrodynamic Boundary Conditions

We assume nonslip conditions at all rigid walls. Furthermore, no mass is transported over the cylinder surface:

$$u = v = 0|_{x=B/2,\,y=0,\,y=H} \wedge u = 0|_{x=0} \wedge u_r = 0|_{r=R} \wedge \frac{\partial v}{\partial x} = 0\bigg|_{x=0} \tag{8}$$

Applying Newton's law of viscosity and considering the fact that $\tau_g \ll \tau_l$, a balance between viscous shear stresses and surface tension forces on the free surface in the azimuthal direction yields the so-called Marangoni boundary condition [5]:

$$\tau_l + \tau_g \approx \tau_l \approx \frac{1}{R}\frac{\partial \sigma}{\partial \varphi} \approx \frac{1}{R}\frac{\partial T}{\partial \varphi}\frac{d\sigma}{dT} \approx \eta\left(\frac{\partial u_\varphi}{\partial r} - \frac{u_\varphi}{r}\right)\bigg|_{r=R} \tag{9}$$

Initially, the liquid in the container is at rest, and the temperature distribution is described by a linear profile in the y direction with isothermal cross sections for y = const, equivalent to steady state heat conduction in a box with isothermal top and bottom and adiabatic side walls.

TEMPERATURE COEFFICIENT OF SURFACE TENSION

The temperature dependence of surface tension $\sigma = \sigma(T)$ is the important impetus for thermocapillary convection. In general, the temperature coefficient of surface tension $d\sigma/dT$ in Eq. (9) is negative. However, for some liquid metals and alloys [10], and some aqueous solutions of alcohols [11], positive gradients are reported.

Based on van der Waals's equation [12], Rathjen and Straub [13] developed a universal relation for the temperature dependence of surface tension with fluid-specific constants σ_0, μ, γ, and T_c. Straub et al. [14] evaluated these constants in a separate study for water:

$$\sigma = \sigma_0\left(1 - \frac{T}{T_c}\right)^{\mu}\left[1 + \gamma\left(1 - \frac{T}{T_c}\right)\right] \tag{10}$$

Differentiation yields the temperature coefficient of surface tension as a function of T:

$$\frac{d\sigma}{dT} = -\frac{\sigma_0}{T_c}\left(1 - \frac{T}{T_c}\right)^{\mu}\left[\mu\left(\frac{T_c}{T_c - T}\right) + \gamma(1 + \mu)\right] \tag{11}$$

We used water at a mean temperature of 365 K as a test fluid in our calculations, even if for some other reason, Marangoni convection is not always observed in water [5]. One reason for the use of this test fluid is that the thermophysical properties are easily available, in particular, the properties of surface tension are well known for a wide region. It is also interesting to investigate to what extent

Marangoni flow in pure water could be induced because it is known from experimental work [15] that Marangoni flow in water is highly affected by the purity of the liquid surface. Furthermore, the Prandtl number of this test fluid is about 2, which is representative for many fluids in practical use. Nevertheless, it is necessary in the future to examine in detail the influence of the Prandtl number on heat transfer and fluid flow.

The small temperature differences up to 1.7 K from the mean temperature of the liquid, and the great distance to the critical point, justify the use of a constant temperature gradient of surface tension for the given conditions. A series of calculations was performed to examine the influence of a constant and a variable temperature coefficient of surface tension. The deviations in the steady state overall Nusselt number between calculations with $d\sigma/dT = d\sigma/dT(T)$ and $d\sigma/dT = \text{const}$ are less than 0.01%.

The thermophysical properties of the test liquid are shown in Table 1. Constant properties are used because the biggest temperature differences in the system under consideration did not exceed 3.4 K in a range of $0 < \text{Ma} \leq 250{,}000$.

MATHEMATICAL MODEL

As no analytical solution of the problem under consideration is possible, the governing equations are integrated numerically using a control volume finite difference method. Implicit and semi-implicit numerical methods are frequently preferred to explicit schemes in transient fluid flow calculations, since time steps of arbitrary size can be chosen. However, their computational effort is greater, and sometimes an iterative solution is necessary. Explicit methods, on the other hand, can easily be implemented, and their computational simplicity can make up for the limitation of the time step by stability criteria. In particular, when the focus is on the transient development of a flow, explicit methods are preferable. Moreover, our experience of several years with explicit finite difference schemes favored the use of this method.

COMPUTATIONAL GRID

The special combination of a circular and a rectangular geometry excludes the use of a regular computational grid. Resorting to a well-tested computer code for transient heat transfer and fluid flow problems in rectangular or cylindrical

Table 1. Thermophysical Properties of the Test Liquid (Pr = 1.93)

	Value	Unit of Measure
c_p	4206.9	J/kg K
λ	0.673	W/m K
η	308.64×10^{-6}	Ns/m^2
ϱ_0	963.84	kg/m^3
β_p	7.116×10^{-4}	1/K
$d\sigma/dT$	-1.8892×10^{-4}	N/m K

calculation domains [7, 16] with finite control volumes, various difference schemes [17, 18], and explicit time steps, the circular geometry of the cylinder and the rectangular cavity in Figure 1 were discretized using "blocked-off regions" [17] in connection with regular triangular elements. Temperature and pressure are calculated in the center of a control volume of this grid, which is therefore denoted "energy grid" (Figure 2). For the velocities, a "staggered" or "displaced" grid [17] is utilized. Based on the procedure described by Patankar [17] for rectangular control volumes, modified balances for energy and momentum can easily be obtained for the nonrectangular elements.

CHOICE OF GRID SIZE

For the selection of the grid size, contradictory arguments had to be considered. On the one hand, an efficient simulation regarding the computing time is desirable; on the other hand, a precise approximation of the cylinder surface and discretization of the whole calculation domain are necessary for accurate results.

Therefore, test simulations starting with 10×20 up to 80×160 control volumes in the rectangular calculation domain of Figures 1 and 2 were performed to establish the necessary grid refinement. The temperature distribution and the velocity profile around the cylinder became grid independent for a grid with 40×80 control volumes or finer for several examined configurations, Marangoni numbers, and gravity levels, presented as case studies below. For higher Marangoni numbers, oscillations occurred in the velocity and temperature profiles. Even these oscillations, observed in terms of the transient development of the integral Nusselt number at the heated and cooled walls, were grid independent for grids 40×80 or finer.

Nevertheless, for security purposes, a grid of 50×100 control volumes was eventually chosen for the simulations (discussed below). With this grid, the average computing time on a Cray Y-MP 4/432 supercomputer amounted to about 1000 CPU seconds for a given Marangoni number.

STABILITY CRITERIA OF THE EXPLICIT METHOD

In the discretized explicit form of the conservation laws for energy and momentum, the size of the time step Δt has to be chosen within a fixed limit. Otherwise, physically unrealistic results or instabilities in the computer code are induced. The diffusive stability criterion derives from the second law of thermodynamics [17, 19], while the convective limit is given by the Courant-Friedrichs-Lewy (CFL) condition [19]. The admissible time step Δt_{max} is the minimum time step resulting from both criteria [19]. We additionally employed a security factor S for the choice of the time step:

$$\Delta t = \frac{1}{S} \Delta t_{max} \tag{12}$$

Examining the influence of this security factor on the calculated results and the required computing time, pure thermocapillary convection around a gas cylinder

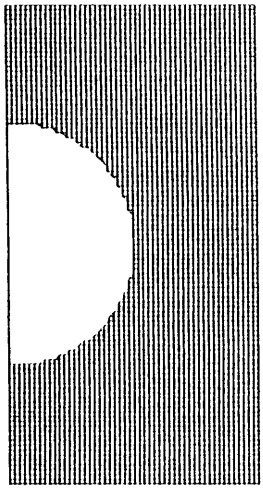

Figure 2. "Energy grid" with 50×100 control volumes.

was studied with S as a parameter until steady state conditions were reached. For increasing S ($S \geq 1$) the value of the overall Nusselt number in the system stabilized, especially for $S \geq 3.0$. The computing time exhibits a minimum for $S \approx 1.25$. For $S > 5$, a large consumption of CPU time was observed because of frequent calls of the subroutines for energy and momentum.

Owing to the rapid convergence of the solution for $S \geq 3.0$ and the large consumption of CPU time for $S > 5.0$, we chose a security factor of $S = 4.0$ for the determination of the time step.

PRESSURE-VELOCITY ITERATION

The numerical integration of the momentum equations involves the difficulty that only the pressure for the old time level p^+ is available, which is in general, different from the pressure for the new time level. According to Patankar [17], an equation for the pressure correction p' is obtained from the momentum and mass conservation equations. Instead of solving the complete pressure correction equation like Patankar, Wengle [18] proposes that the influence of the mass source b is more decisive than that of the unknown pressure corrections of the neighboring grid points p'_{nb}. Neglecting the latter, p'_P can be directly calculated:

$$p'_P \approx \frac{b}{a_P} \tag{13}$$

The required computing time for the pressure-velocity method proposed by Wengle is relatively small when explicit time steps are used.

With corresponding relaxation factors ω_p and ω_v, updated values for the pressure p^{**} and the velocities u^{**} and v^{**} are calculated from the correction values:

$$p^{**} = p^{*} + \omega_p p' \wedge u^{**} = u^{*} + \omega_v u' \wedge v^{**} = v^{*} + \omega_v v' \tag{14}$$

For implicit schemes, underrelaxation is necessary with $\omega_p \leq 0.8$ and $\omega_v \leq 0.5$ [17] in order to enable convergence of the pressure-velocity iteration. On the other hand, underrelaxation slows down the rate of convergence due to its dampening effect. A speed-up is highly desirable, which is possible by overrelaxation with an explicit method. For our explicit scheme, good convergence was obtained for $\omega_p > 1.0$ and $\omega_v > 1.0$. A hybrid relaxation proposed in the MAPLE algorithm by Marek and Straub [20] reduces the number of necessary iterations by employing alternately underrelaxation ($\omega < 1$) and overrelaxation ($\omega > 1$), depending on the convergence or divergence of the previous iteration step.

OTHER PRESSURE-VELOCITY ALGORITHMS

Searching for an efficient pressure-velocity correction, we investigated two more algorithms for solving the pressure correction equation, where the pressure corrections of the neighboring points are considered: the SIMPLE algorithm with tridiagonal matrix algorithm (TDMA) solver [21, 22] and the SIMPLEC algorithm with TDMA solver [21, 23].

The iterative solution of the pressure correction equation with the TDMA-SIMPLE algorithm consumed only half of the computing time of the MAPLE algorithm in the early stage of the flow for obtaining results of comparable accuracy. However, when the fluid field approached its steady state, the computational effort of the TDMA method increased enormously. As the savings in computing time existed only in the beginning of the computation, the SIMPLE algorithm with TDMA solver was not employed. A similar result occurred for the TDMA-SIMPLEC algorithm.

RESULTS

Decaying Flow Behavior

Varying Ma and Ra via the temperature gradient in the container, we performed case studies of Marangoni convection and the corresponding heat transfer around the gas cylinder for some selected configurations (Figure 3), under both microgravity and Earth's gravity conditions.

Case M: Pure Marangoni convection (M) around a gas cylinder in the center of a 2D container under microgravity ($g \approx 0$).

Case M − B: Marangoni flow acting against buoyancy convection (M − B) around a gas cylinder frozen in the center of a 2D container under Earth's gravity ($\partial T/\partial y > 0$).

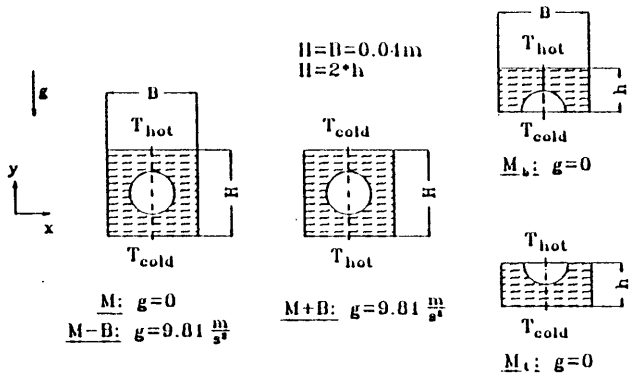

Figure 3. Overview of studied configurations: cases M, M − B, M + B, M_b, and M_t.

Case M + B: Marangoni convection acting in the direction of buoyancy flow (M + B) around a gas cylinder frozen in the center of a 2D container under Earth's gravity ($\partial T/\partial y < 0$).

Case M_b: Pure Marangoni convection (M) around a semicircular cylinder on the bottom wall of a flat container under microgravity ($g \approx 0$).

Case M_t: Pure Marangoni convection (M) around a semicircular cylinder on the top wall of a flat container under microgravity ($g \approx 0$).

Due to lack of space here, only steady state results are presented for cases M − B through M_t, although the transient development of the flow and temperature fields has been fully investigated.

The rigid container walls give rise to a recirculating flow in the liquid, illustrated in Figures 4–6 together with the corresponding isotherms. All velocity vectors are related to the maximum velocity occurring in the system; thus comparisons between different flow patterns cannot necessarily be drawn.

The temperature field around the cylinder is strongly coupled with the flow field. When the Marangoni number or the temperature difference between bottom and top walls of the container, respectively, is increased, the influence of thermocapillary convection on heat transfer grows, and the isotherms accumulate near the heated and cooled walls, which is equivalent to an increase in the local and global Nusselt numbers at those walls. The number of isotherms originating from the cylinder surface decreases with increasing Marangoni number (Figures 4–6), which is in accordance with Ref. [5]. The computations thus clearly account for the effect that Marangoni convection reduces its own driving temperature gradients.

The behavior of Marangoni convection under Earth's gravity conditions is very noticeable. In case M − B, a stable vertical density stratification is initially present in the enclosure. The displacement of the isotherms in Figure 5*a* demonstrates the effect that Marangoni convection exerts on buoyancy flow. For $d\sigma/dT < 0$, fluid particles are driven against the direction of natural convection, and this

flow pattern still prevails when the number of isotherms originating from the free surface is reduced at higher Marangoni numbers. Recently, Straub et al. [5] presented some experimental results for this phenomenon. On the other hand, compared with microgravity conditions (Figure 4), buoyancy displaces the bulk flow toward the cylinder surface. In case M + B, an unstable density stratification is chosen as the initial condition in the box, so that Marangoni and buoyancy convection augment each other. Due to the reversed temperature gradient in the enclosure, surface tension driven convection acts in the opposite direction in comparison with cases M and M − B. Figure 5*b* illustrates that, even for small Marangoni numbers, the recirculating flow pattern prevails over a large part of the liquid.

For small Marangoni numbers, the absolute velocities in the liquid are very moderate; hence diffusive heat transfer is dominant over convective energy transport. The insulating effect of the gas cylinder reduces the heat transfer in the enclosure to 67.5% of the value for pure steady state heat conduction in a box of the same size without a cylinder and only filled with liquid, which was defined as the initial condition for Fo = 0 earlier. This behavior is depicted in Figure 7 (Ma = 10). We scaled all Nusselt numbers with the reference value for steady state

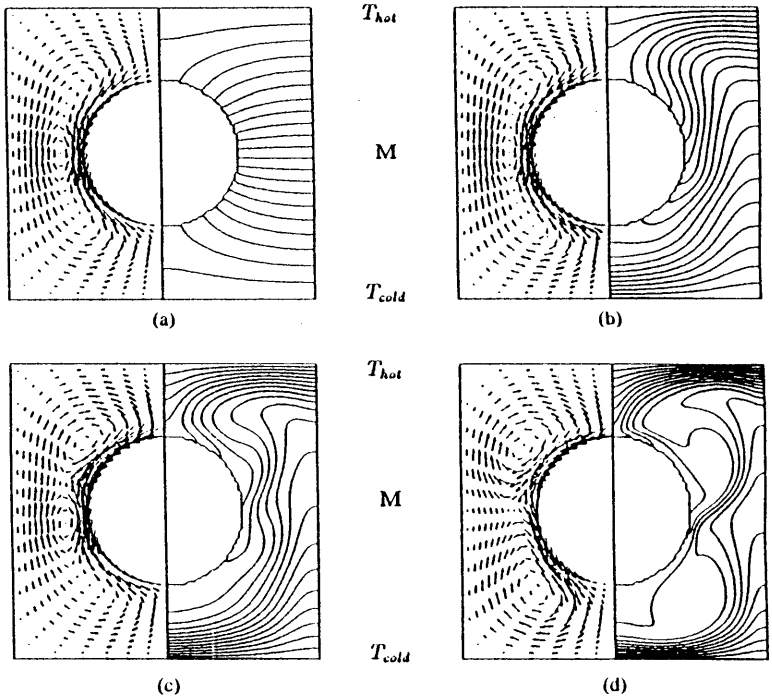

Figure 4. Predicted velocity fields and isotherms for case M: (a) Ma = 10, (b) Ma = 5,000, (c) Ma = 10,000, (d) Ma = 100,000, Ra = 0.

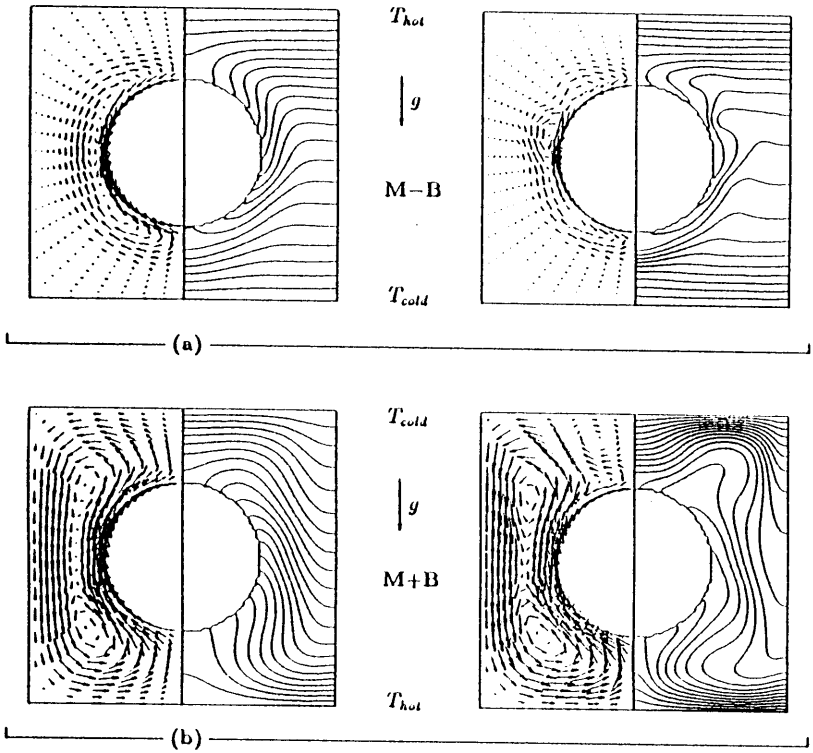

Figure 5. Predicted velocity fields and isotherms for (a) case M − B: Ma = 10,000, Ra = 5.7×10^5 (left), Ma = 100,000, Ra = 5.7×10^6 (right), and (b) case M + B: Ma = 1,000, Ra = 5.7×10^4 (left), Ma = 5,000, Ra = 2.8×10^5 (right).

heat conduction in a box with a cylinder, shown in Figure 1 (Nu = 1.0). The reduction of heat transfer by 32.5% in the case of pure heat conduction (Ma → 0) was obtained by both the 2D flow calculation described above (Figure 4) and by employing a control volume finite element method proposed by Baliga and Patankar [24]. Furthermore, the calculated results agree with an investigation by Riedle et al. [25].

For a growing Marangoni number, convection dominates heat conduction, resulting in an increase of the integral Nusselt number at the heated and cooled walls for Fo > 0 (Figure 7). For Ma > 5×10^3, an overshooting of the flow at the beginning of the calculations causes damped oscillations in the Nusselt numbers at the bottom and the top, vanishing in the steady state. It should be pointed out that the amplitude of the oscillation is higher on the cold side of the cavity than on the hot side. This effect may be explained by the fact that the flow is pushed toward the cold side.

In order to demonstrate the enhancement of the heat transfer in the box by thermocapillary convection, the steady state integral Nusselt number Nu at the isothermal bottom and top walls is depicted as a function of the Marangoni number Ma for cases M through M_t in Figure 8. Nu at the isothermal container walls increases with growing Ma for all cases investigated. However, for higher Ma this increase in Nu becomes smaller. The reason for this behavior is the reduction of the important temperature gradients near the free surface by Marangoni convection itself, which occurs to a much greater extent for high Marangoni numbers.

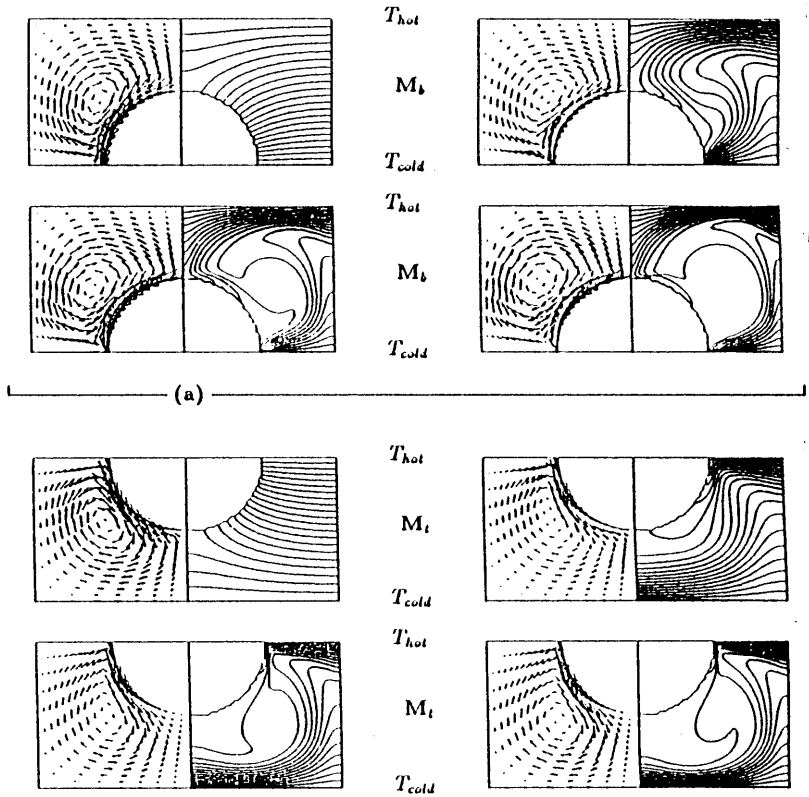

Figure 6. Predicted velocity fields and isotherms for (a) case M_b: Ma = 10 (left top), Ma = 10,000 (right top), Ma = 50,000 (left bottom), Ma = 250,000 (right bottom), Ra = 0, and (b) case M_t: Ma = 10 (left top), Ma = 5,000 (right top), Ma = 25,000 (left bottom), Ma = 50,000 (right bottom), Ra = 0.

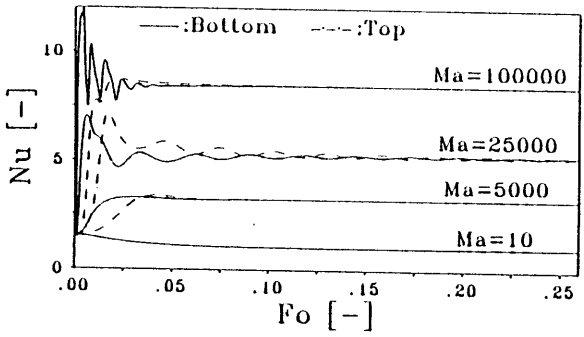

Figure 7. Transient development of the Nusselt number at the isothermal bottom and top walls for case M and several Marangoni numbers.

Oscillatory Flow Behavior

For Marangoni numbers Ma > Ma_{osc} (Table 2a), neither a steady state flow pattern nor a constant temperature distribution in the calculation domain could be obtained for cases M, M + B, and M_t. In the transient plot of the Nusselt number Nu = Nu(t), a stable oscillation around a mean value $\overline{Nu}$ (Figures 9*a* and 9*b*) occurred for these cases. Therefore, the average value $\overline{Nu}$, calculated for the steady state case, was used for the curves in Figure 8. The Nusselt numbers for the bottom and top walls averaged in such a manner were identical, indicating that the first law of thermodynamics is satisfied for the whole container.

At first sight, one might suppose that the oscillatory behavior is induced by the explicit method applied. Therefore a series of modifications of the source code

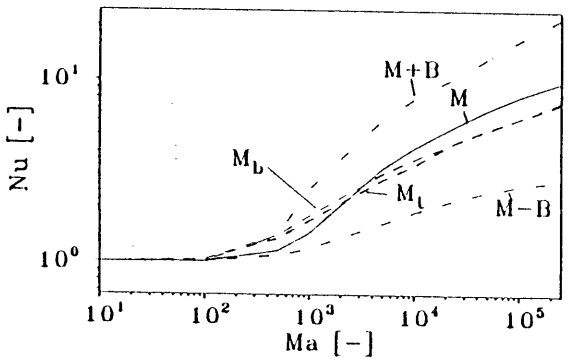

Figure 8. Overall steady state Nusselt number Nu at the isothermal walls of the container as a function of the Marangoni number Ma for the cases investigated (Pr = 1.93).

Table 2. Reynolds Numbers Re for the Container and Corresponding Marangoni Numbers Ma (a) for the Onset of Oscillatory Flow (Ma_{osc}) in Cases M, M + B, and M_t, and (b) for the Stable Flow Modes of Cases M − B and M_b (Ma = 250,000)

Case	Ma_{osc}	Re	Case	Ma	Re
M	250,000	507.7	M − B	250,000	491.0
M + B	5,000	53.0	M_b	250,000	811.7
M_t	100,000	605.8			
	(a)			(b)	

was performed; however, the oscillations were not affected by any of the following factors: the use of various security factors S in the time step module; variation of the admissible mass source b_{max} per control volume; employing central difference, upwind, or hybrid finite differences instead of the employed power law scheme [17] in the discretized energy and momentum equations; employing a finer grid; or

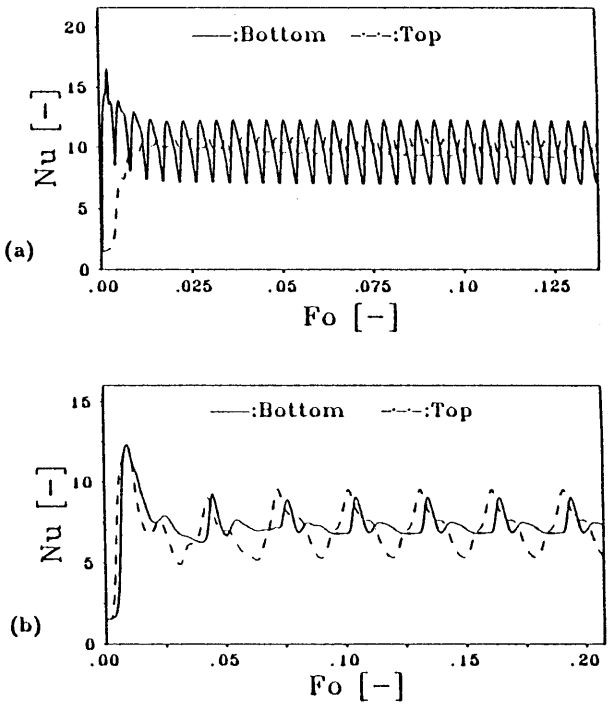

Figure 9. Oscillatory transient development of the Nusselt number at the isothermal walls for (a) case M, Ma = 250,000, $g \approx 0$ and (b) case M + B, Ma = 10,000, Ra = 5.7×10^5.

using double-precision variables on the Cray Y-MP 4/432. Hence, round-off errors, discretization errors, and errors deriving from improper time steps can be excluded as possible reasons for the oscillatory behavior.

As the Reynolds number Re in the enclosure did not exceed 1,000 (Table 2), the fluid flow is supposed to be laminar for all cases studied. From Table 2 no direct relationship between Re, or the maximum velocity in the container w_{max}, and the observed oscillations can be derived.

As Roache [19] points out, the numerical integration of the governing equations of unsteady heat transfer and fluid flow yields unstable solutions for vanishing diffusive dampening terms α and η ($\alpha \to 0, \eta \to 0$), when central differences and explicit time steps are used. In the problem under consideration, the dampening terms in the conservation laws are missing at the free surface of the liquid, too, but for the employed power law, upwind, and hybrid schemes, no instability effects have been reported so far.

Real physical effects should be taken into account, as well. Marangoni convection is strongly coupled with the temperature field on the free surface of the gas cylinder, and reduces, on the other hand, the temperature gradients by the induced flow. This mechanism can theoretically cause oscillations in the temperature and flow fields in the vicinity of the free surface, as simulated numerically here for a few cases and Marangoni numbers. Moreover, the work of other authors about oscillatory thermocapillary convection supports the above findings. Villers and Platten [26] observed oscillatory flows in a 2D box with a free surface both experimentally and numerically for high Ma and Ra numbers. For liquid columns, several works refer to the existence of oscillatory thermocapillary convection, e.g., [27–29]. However, the physical background for the formation of oscillations has not been clear up to now. Nevertheless, numerical instabilities should not be excluded completely. They can appear in free-surface regions, in general, and at locations where the Marangoni condition acts abruptly, like at the head and bottom of the gas bubble. Here, the strong coupling of energy and momentum equations can stimulate oscillations.

CONCLUSION

In the previous section, the enhancement of heat transfer in a rectangular container by thermocapillary convection was established quantitatively in terms of the steady state Nusselt number Nu and the Marangoni number Ma for some selected cylinder-in-container configurations and a liquid with Pr = 1.93. The obtained findings once more clearly emphasize the importance of thermocapillary convection on heat transfer in liquids both under microgravity and Earth's gravity.

Future investigations will focus on a universal description of the enhancement of heat transfer by Marangoni convection with dimensionless quantities Marangoni, Fourier, Rayleigh, Nusselt, Prandtl, and Froude obtained from the dimensionless conservation laws for energy and momentum.

Parameters not, or only partially, considered as yet are the size of the cylinder and the box (ratio R/H), its location in the container, the physical properties of the liquid (Pr), the ratio of natural and Marangoni convection (Bond number Bo = Ra/Ma), and the geometry of the container (ratio H/B).

Furthermore, the oscillatory flow behavior in the liquid is to be examined more exactly; the physical background for the oscillations especially must be elucidated systematically. At present, work is in progress to derive comparisons between the results obtained with the presented explicit numerical method and solutions delivered by a transient program code using control volume finite element discretization with implicit time steps, developed after the concepts of Baliga and Patankar [24] and Prakash and Patankar [30]. The comparisons show very good agreement between the two different numerical methods, and support the above findings.

REFERENCES

1. C. G. M. Marangoni, Ueber die Ausbreitung der Tropfen einer Flüssigkeit auf der Oberfläche einer anderen, *Ann. Phys. Chem.*, vol. 143, no. 7, pp. 337–354, 1871.
2. C.-H. Chun, Numerical Study on the Thermal Marangoni Convection and Comparison with Experimental Results from the TEXUS-Rocket Program, *Acta Astronaut.*, vol. 11, nos. 3–4, pp. 227–232, 1984.
3. P. Hammerschmid, Bedeutung des Marangoni-Effekts für metallurgische Vorgänge, *Stahl Eisen*, vol. 107, no. 2, pp. 61–66, 1987.
4. J. Martinez, J. M. Haynes, and D. Langbein, Fluid Statics and Capillary in Fluid Science and Material Science in Space, in H. U. Walter (ed.), *Fluid Sciences and Material Sciences in Space*, Springer Verlag, New York, 1987.
5. J. Straub, A. Weinzierl, and M. Zell, Thermokapillare Grenzflächenkonvektion an Gasblasen in einem Temperaturgradienten, *Thermo Fluid Dyn.*, vol. 25, pp. 281–288, 1990.
6. N. O. Young, J. S. Goldstein, and M. J. Block, The Motion of Bubbles in a Vertical Temperature Gradient, *J. Fluid Mech.*, vol. 6, pp. 350–356, 1959.
7. R. Marek and J. Straub, Three-Dimensional Transient Simulation of Marangoni Flow in a Cylindrical Enclosure under Various Gravity Levels, *Microgravity Sci. Technol.*, vol. 4, no. 2, pp. 153–154, 1991.
8. J. V. Boussinesq, Théorie Analytique de la Chaleur, vol. 2, Gauthier-Villard, Paris, 1903.
9. B. R. Bird, W. E. Stewart, and E. N. Lightfoot, *Transport Phenomena*, John Wiley, New York, 1960.
10. P. J. Desre and J. C. Joud, Surface Tension Temperature Coefficient of Liquid Alloys and Definition of a "Zero Marangoni Number Alloy" for Crystallization Experiments in Microgravity Environments, *Acta Astron.*, vol. 8, pp. 407–415, 1981.
11. J. De Coninck, D. Villers, and J. K. Platten, Nonmonotonous Temperature Dependence of Interfacial Tensions, *J. Phys. Chem.*, vol. 94, no. 12, pp. 5057–5059, 1990.
12. J. D. van der Waals, Die thermodynamische Theorie der Kapillarität unter Voraussetzung stetiger Dichteänderung, *Z. Phys. Chem.*, vol. 13, pp. 657–725, 1894.
13. W. Rathjen and J. Straub, Die Temperaturabhängigkeit der Oberflächenspannung von reinen Kältemitteln vom Tripelpunkt bis zum kritischen Punkt, *Thermo Fluid Dyn.*, vol. 14, pp. 59–73, 1980.
14. J. Straub, N. Rosner, and U. Grigull, Oberflächenspannung von leichtem und schwerem Wasser, *Thermo Fluid Dyn.*, vol. 13, pp. 241–251, 1980.
15. A. Ito, S. K. Choudhury, and T. Fukano, Heated Liquid Film Flow and Its Breakdown Caused by Marangoni Convection (the Characteristic Flow of Pure Water), *JSME Int. J., Ser. II*, vol. 33, no. 1, pp. 128–133, 1990.
16. A. Heiss, Numerische und experimentelle Untersuchungen der laminaren und turbulenten Konvektion in einem geschlossenen Behälter, dissertation, Lehrstuhl A für Thermodynamik, Technical University of Munich, 1987.

17. S. V. Patankar, *Numerical Heat Transfer and Fluid Flow*, Hemisphere, Washington, D.C., 1980.
18. H. Wengle, Diskretisierung der dreidimensionalen und zeitabhängigen Navier-Stokes-Gleichungen für ein stark dichteveränderliches Fluid, Hochschule der Bundeswehr München, report no. 1/82/1, Neubiberg, 1983.
19. P. J. Roache, *Computational Fluid Dynamics*, Hermosa, Albuquerque, N. Mex., 1976.
20. R. Marek and J. Straub, Hybridrelaxation—A Technique to Enhance the Rate of Convergence of Iterative Algorithms, *Numer. Heat Transfer, Part B: Fundamentals*, 1993 (in press).
21. J. P. van Doormaal and G. D. Raithby, Enhancements of the SIMPLE Method for Predicting Incompressible Fluid Flows, *Numer. Heat Transfer*, vol. 7, pp. 147–163, 1984.
22. S. V. Patankar, A Calculation Procedure for Two-Dimensional Elliptic Situations, *Numer. Heat Transfer*, vol. 4, pp. 409–425, 1981.
23. D. S. Jang, R. Jetli, and S. Acharya, Comparison of the PISO, SIMPLER and SIMPLEC Algorithms for the Treatment of the Pressure-Velocity Coupling in Steady Flow Problems, *Numer. Heat Transfer*, vol. 10, pp. 209–228, 1986.
24. R. B. Baliga and S. V. Patankar, A Control Volume Finite-Element Method for Two-Dimensional Fluid Flow and Heat Transfer, *Numer. Heat Transfer*, vol. 6, pp. 245–261, 1983.
25. K. Riedle, H. Sebulke, and U. Grigull, Formkoeffizient des Wärmestroms in gelochten Flanschen und Streifen, *Thermo Fluid Dyn.*, vol. 3, pp. 70–74, 1970.
26. D. Villers and J. K. Platten, Coupled Buoyancy and Marangoni Convection in Acetone: Experiments and Comparison with Numerical Simulations, *J. Fluid Mech.*, vol. 234, pp. 487–510, 1992.
27. Ch. H. Chun and W. Wuest, Experiments on the Transition from the Steady to the Oscillatory Marangoni Convection of a Floating Zone under Reduced Gravity, *Acta Astronaut.*, vol. 6, no. 9, pp. 1073–1082, 1979.
28. D. Schwabe, R. Velten, and A. Scharmann, The Instability of Surface Tension Driven Flow in Models for Floating Zones under Normal and Reduced Gravity, *J. Crystal Growth*, vol. 99, pp. 1258–1264, 1990.
29. R. Rupp, G. Mueller, and G. Neumann, Three-Dimensional Time Dependent Modelling of the Marangoni Convection in Zone Melting Configurations for GaAs, *J. Crystal Growth*, vol. 97, pp. 34–41, 1989.
30. C. Prakash and S. V. Patankar, A Control Volume-Based Finite-Element Method for Solving the Navier-Stokes Equation Using Equal-Order Variable Interpolation, *Numer. Heat Transfer*, vol. 8, pp. 259–280, 1985.